The Formation of an Epitax between Silver Carboxylates and Silver Bromide in the Initial Stages of Silver Soap Crystallization

D. R. Whitcomb, Eastman Kodak Company, Oakdale, MN,/USA; J. Dong, B. Lin, A. McCormick, H. T. Davis, University of Minnesota, MN/USA

Abstract

The presence of an epitaxial interface between the silver carboxylate and silver bromide nanocrystals in photothermographic imaging materials has been debated for many years. This type of an interface has been observed in model systems, and the reaction conditions used to prepare the silver soap (in the presence of the silver bromide) are conducive to the formation of that interface. In order to determine if this interface can be detected at any stage of formation of the silver soap during its preparation in the presence of silver bromide nanocrystals, we have undertaken cryogenic TEM investigations to freeze the reaction and reveal the formation of the silver stearate (AgSt) microstructure at the very initial stages of the reaction, which precedes significant crystal lattice formation. We found 5 nm-sized AgSt micelles, which aggregate to produce larger (50–100 nm in size), loosely packed crystals, but AgSt nucleates on AgBr when 50 nm cubic grains are added to the NaSt dispersion prior to the AgNO₃. After nucleation, the AgSt micelles form structures via an epitaxial interface on at least one corner of every available AgBr cubic crystal. Complete details of this reaction process and the implications to subsequent silver soap crystal growth will be discussed in this talk.

Introduction

Silver complexes of long chain fatty acids have been utilized for a long time in thermographic and photothermographic imaging materials [1–3]. The preparation of the silver carboxylate (soap) component of these imaging materials has been the subject of many patents [see for example, 4–6] but very little has been reported in the literature regarding the functional details of this process [7–10] Of particular interest here is how the silver soap forms in the presence of a nucleating site, such as the nano-particles of silver bromide [11]. In this case, the formation of an epitaxial interface between the dissimilar crystal lattices of the silver bromide and the silver carboxylate has been the subject of literature debate, especially as its potential involvement in modifying the photophysics of the imaging process [12,13]. The importance of this interface is fundamental to the postulate that it is the basis for the photocatalytic mechanism of latent image formation in PTG materials [15,16]. It explains the silver halide grain size independence of photocharge signals observed in systems in which this type of interface can form, as well as the observation that conventional silver halide chemical sensitization methods do not seem to work well in solvent-based PTG formulations. A better understanding of this silver soap crystallization process should be useful in improving the imaging properties of imaging materials made from it.

The object of this study is to reveal the details of the initial stages of reaction of the silver ion with the sodium soap in order to understand the processes involved that control the formation of the final silver carboxylate crystal, and to determine to what extent an epitaxial interface is formed between the silver bromide nanocrystals and the silver soap formed in its presence. We now report that silver soap crystallization dominates over crystal growth and large numbers of size-limited silver carboxylate crystals form. In the presence of cubic silver bromide nanocrystal grains, clear evidence for the crystallization of silver stearate via an epitax on every silver bromide grain was obtained. The details of this investigation and conclusions are given below.

Experimental

On-the-grid reaction was carried out by mixing sodium stearate (NaSt, >99%; Sigma Chemical Co., MO) and silver nitrate (AgNO₃, Allied Chemical Co., NJ) directly on a TEM grid supporting a perforated carbon film (Ted Pella, Inc.: hole sizes range 1–10 µm in diameter), as described elsewhere [17,18]. The reaction was then quenched by plunging the specimen into liquid ethane at its melting point cooled by liquid nitrogen [19]. The vitrified specimen was mounted on a Gatan cryo-holder and transferred into a JEOL 1210 TEM. All images were recorded with a Gatan 724 MultiScan camera at –170 °C. High magnification images were obtained with low electron doses (fewer than 10 electrons/$\AA^2$) to minimize electron-beam radiation damage to the specimen [19].

Results and Discussion

Characterization of the Initial Stages of the Reaction between Silver Nitrate and Sodium Stearate

The addition of silver ion to the sodium soap under normal conditions is usually carried out below the sodium soap Krafft temperature (temperature-limited solubility boundary). Consequently, the sodium soap is not a solution but a dispersion of crystals. Thus, it is important to first establish if the solid-state structure of the sodium soap ribbon has any effect on the solid-state structure of the resulting silver soap. Optical microscopy shows that the initial NaSt crystallites (on the order of $10–20 \times 1–5 \times 0.5–1$ µ) are primarily ribbons below the Krafft temperature. We found that within the first 15–20 min the silver stearate could be observed at room temperature to undergo normal Ostwald ripening processes. However, higher magnification was needed to see the details regarding the AgSt formation, particularly at the very initial stages of crystallization. Cryo-TEM enables an aqueous sample to be prepared and flash-vitrified when placed on a TEM viewing grid [19]. Representative cryo-TEM images of 10 s reaction times are shown in Figure 1. These AgSt aggregates are generally around 50 nm in size.
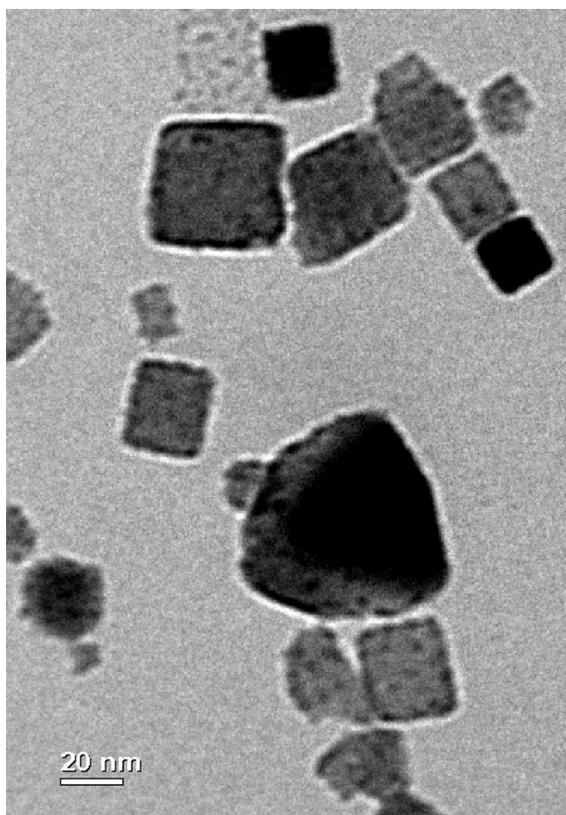
Figure 1. [(C$_{18}$H$_{35}$O$_2$)$_x$(Na$_{x-y}$)(Ag$_y$)(H$_2$O)$_z$] micelle aggregation.

In addition to the aggregates, many small "dots" less than 5 nm in size are also visible. All of the aggregates, large or small, are comprised of many of these much smaller, 5 nm particles loosely packed together. We propose that these dots are the very initial silver soap micelles having a mixed composition, [(C$_{18}$H$_{35}$O$_2$)$_x$(Na$_{x-y}$)(Ag$_y$)(H$_2$O)$_z$], which is indistinguishable from [(H$_2$O)$_z$AgSt]$_n$ at this stage.

Effect of AgBr Nanocrystals on the Initial Stages of the Reaction between Silver Nitrate and Sodium Stearate

When AgNO$_3$ is added to the NaSt dispersion containing 50 nm AgBr nanocrystals, significant differences are observed. As in the case without AgBr, spherical [(H$_2$O)$_z$AgSt]$_n$ micelles are initially formed. Quite unlike the AgBr-free reaction mixture, however, no subsequent aggregation of those silver stearate micelles was observed over equivalent reaction times. Instead, the AgSt micelles can be observed to adhere to the AgBr crystal surfaces. Initially, the nucleation site on the AgBr grain seems to be non-preferential, multiple deposits are observed over many crystallographic planes on the AgBr (Figure 2), and begin to coalesce into epitaxial buds.
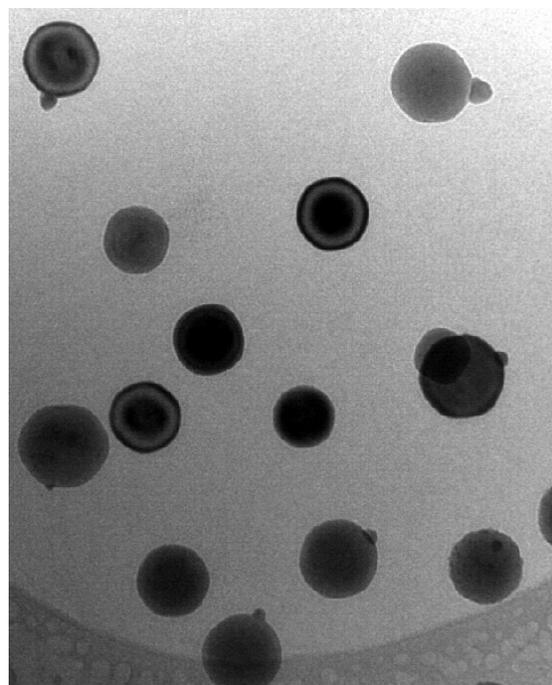
Figure 2. Silver stearate deposition on AgBr (50 nm) grains

The silver stearate micelle concentration diminishes, and fewer micelles are observed on the silver bromide surface. The composition of the pre-epitax was found by FT-IR to be AgSt crystals (likely retaining some water of hydration at this stage) resulting from subsequent additional deposition of AgSt micelles and Ostwald ripening of the incipient AgSt crystal.

As the reaction time prior to plunge-freezing is increased to 5 min, the AgSt buds become longer, and the first indication of the periodic AgSt lamellar structure begins to appear (Figure 3).
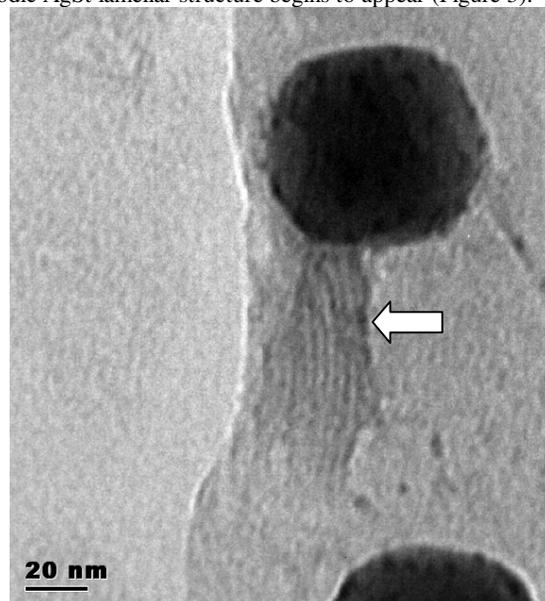
Figure 3. AgSt epitax growth.

As the reaction time proceeds, 10 min and longer, the larger portions of the silver stearate structures then begin to show the well-known plate-like structures.

Conclusions

The initial stage of the reaction between NaSt and $AgNO_3$ produces both AgSt micelles, $[(C_{18}H_{35}O_2)_x(Na_{x-y})(Ag_y)(H_2O)_z]$, and AgSt micelle aggregations that form cubic-shaped pre-AgSt crystals. This is a diffusion-controlled process, and the silver ions react primarily with solvated NaSt molecules and micelles rather than the solid NaSt dispersion. The morphology of the starting sodium soap crystallites has no influence on the morphology of the subsequently formed silver soap crystallites.

When cubic grains of 50 nm AgBr are added to the NaSt dispersion prior to the $AgNO_3$, the exchange reaction proceeds to form the silver stearate micelles, but the presence of the new surface provides a nucleation site that initially short-circuits the aggregation of silver stearate micelles. The (111) silver ion planes of the AgBr cubic crystal corners provide the preferred nucleation sites for silver stearate micelle deposition and crystal growth. After nucleation, the AgSt micelles form bud-like structures on typically one but up to several corners of each AgBr cubic crystal. The buds grow longer and link other available free ends over this reaction time.

References

[1] P.J. Cowdery-Corvan and D.R. Whitcomb, Phothermographic and Thermographic Imaging Materials, Handbook of Imaging Materials, A. Diamond, D. Weiss, Eds., 2001.

[2] D.R. Whitcomb, Phothermographic and Thermographic Imaging Materials, D.R. Whitcomb and Kirk Othmer, Eds., Encyclopedia of Chemical Technology, online edition, 2003.

[3] D.H. Klosterboer, Neblette's Eighth Edition: Imaging Processes and Materials, J.M. Sturge, V. Walworth, and A. Shepp, Eds., Van Nostrand-Reinhold, Ch. 9, 279 (1989).

[4] A. Hatakeyama, EP Pat. 911,692 (1999).

[5] I. Toya and A. Minami, EP Pat. 1,014,178 (2000).

[6] G. Defieuw, P. Janssen, J. Loccufier, and B. Horsten, U.S. Pat. 5,817,598 (1998).

[7] V. Hrust, N. Kallay, and Dj. Težak, Coll. Polym. Sci., 263, 424 (1985).

[8] Yu.E. Usanov and T.B. Kolesova, J. Imag. Sci. Tech., 40, 104 (1996).

[9] V. Hrust, N. Kallay, and Dj. Težak, Coll. Polym. Sci., 263, 424 (1985).

[10] O. Harva and P. Ekwall, Acta Chem. Scand., 2, 713 (1948).

[11] B.B. Bokhonov, L.P. Burleva, D.R. Whitcomb, and M.R.V. Sahyun, Microsc. Res. Tech., 42 152 (1998).

[12] M.R.V. Sahyun, J. Imag. Sci. Tech., 42, 23 (1998).

[13] H. Strijckers, J. Imag. Sci. Tech., 47, 100 (2003).

[14] K. Yamane and S. Yamashita, Int. Cong. Imag. Sci., 2002, Tokyo.

[15] C. Zou, M.R.V. Sahyun, B. Levy, and N. Serpone, J. Imag. Sci. Tech., 40, 94 (1996).

[16] B.B. Bokhonov, L.P. Burleva, D.R. Whitcomb, and M.L. Brostrom, J. Imag. Sci. Tech., 48, 1 (2004).

[17] J. Dong, D.R Whitcomb, A.V. McCormick, and H.T. Davis, Nanotechnology, 16, S592 (2005).

[18] B. Lin, J. Dong, D.R. Whitcomb, A.V. McCormick, and H.T. Davis, Langmuir, 20, 9069 (2004).

[19] Y. Talmon, Modern Characterization Methods of Surfactant Systems, Chapter 5, B. P. Binks, Ed. (Marcel Dekker, New York, 1999)

Acknowledgments

Author Biography

David Whitcomb, B.A., Ph.D., has been investigating the silver chemistry of photothermographic imaging materials since 1989. In 1999, two years after 3M transferred several business units into a new company, the medical imaging business was sold to Eastman Kodak Company. He is currently continuing this silver chemistry research effort, which also includes understanding the optical properties of the metallic silver nanoparticles. He has over 50 technical publications and 19 patents.